The EMBO Journal (2011) 30, 1238–1250 | © 2011 European Molecular Biology Organization | All Rights Reserved 0261-4189/11
www.embojournal.org

THE EMBO JOURNAL

The mitochondrial fission factor dynamin-related protein 1 modulates T-cell receptor signalling at the immune synapse

Francesc Baixauli[1,2], Noa B Martín-Cófreces[1,2], Giulia Morlino[1], Yolanda R Carrasco[3], Carmen Calabia-Linares[1], Esteban Veiga[1,4], Juan M Serrador[5,6] and Francisco Sánchez-Madrid[1,2,6,*]

[1]Servicio de Inmunología, Hospital Universitario de la Princesa, Universidad Autónoma de Madrid, Instituto Investigación Sanitaria Princesa (IIS-IP), Madrid, Spain, [2]Departamento de Biología Vascular e Inflamación, Centro Nacional de Investigaciones Cardiovasculares, Madrid, Spain, [3]Departamento de Inmunología y Oncología, Centro Nacional de Biotecnología, CSIC, Madrid, Spain, [4]Departamento de Biología Molecular y Celular, Centro Nacional de Biotecnología, CSIC, Madrid, Spain and [5]Departamento de Biología Celular e Inmunología, Centro de Biología Molecular Severo Ochoa, UAM-CSIC, Madrid, Spain

During antigen-specific T-cell activation, mitochondria mobilize towards the vicinity of the immune synapse. We show here that the mitochondrial fission factor dynamin-related protein 1 (Drp1) docks at mitochondria, regulating their positioning and activity near the actin-rich ring of the peripheral supramolecular activation cluster (pSMAC) of the immune synapse. Mitochondrial redistribution in response to T-cell receptor engagement was abolished by Drp1 silencing, expression of the phosphomimetic mutant Drp1S637D and the Drp1-specific inhibitor mdivi-1. Moreover, Drp1 knockdown enhanced mitochondrial depolarization and T-cell receptor signal strength, but decreased myosin phosphorylation, ATP production and T-cell receptor assembly at the central supramolecular activation cluster (cSMAC). Our results indicate that Drp1-dependent mitochondrial positioning and activity controls T-cell activation by fuelling central supramolecular activation cluster assembly at the immune synapse.

The EMBO Journal (2011) **30,** 1238–1250. doi:10.1038/emboj.2011.25; Published online 15 February 2011
Subject Categories: immunology; structural biology
Keywords: cell signalling; fission factor; immune synapse; mitochondria; T-cell receptor

Introduction

Mitochondria regulate many cell processes, including calcium signalling, apoptosis and cell metabolism (McBride *et al*, 2006). The activity of mitochondria is regulated, among others, by their number, shape and positioning (Chen and Chan, 2005). Understanding of mitochondrial function was increased by the finding that mitochondria form a highly dynamic tubular network that is continuously remodelled by opposing processes of fusion and fission (Chan, 2006). Mitochondrial fission and fusion is controlled by a family of highly conserved dynamin-related GTPases. Constriction and fission are driven by hFis and the mitochondrial fission factor dynamin-related protein 1 (Drp1) (Smirnova *et al*, 2001; James *et al*, 2003). Drp1 is a cytosolic protein that forms oligomers that can be recruited to the outer mitochondrial membrane (OMM) by receptors such as hFis, and constricts the organelle in a GTPase-dependent manner (Fukushima *et al*, 2001; Zhu *et al*, 2004). Tethering and fusion of mitochondria are mediated by mitofusins 1 and 2, located in the OMM, and optic atrophy 1 in the intermembrane space, closely associated with the inner mitochondrial membrane (Eura *et al*, 2003; Koshiba *et al*, 2004).

Although the precise function of mitochondrial dynamics is still obscure, recent evidence suggests that the network organization of mitochondria facilitates the propagation of calcium waves and the exchange of molecules such as metabolites, DNA and enzymes from healthy to dysfunctional mitochondria (Chen *et al*, 2005). Fission is also required for the proper distribution of mitochondria to daughter cells during mitosis (Taguchi *et al*, 2007), the selective targeting of damaged mitochondria to autophagy (Twig *et al*, 2008), and the control of mitochondrial distribution within cells (Li *et al*, 2004; Varadi *et al*, 2004; Campello *et al*, 2006).

Mitochondrial concentration at sites of high ATP demand appears to be especially important in highly polarized cells. For example, the positioning of mitochondria in the uropod of polarized lymphocytes and presynaptic axon terminals is essential for fuelling chemotaxis and neurotransmission, respectively (Morris and Hollenbeck, 1993; Campello *et al*, 2006). Mitochondria also seem to regulate neural synapse activity, synaptic plasticity and neurotransmitter release (Verstreken *et al*, 2005).

Immune cells form specialized membrane-based structures that favour transient cell–cell communication. The immune synapse (IS) is a dynamic, polarized macromolecular structure formed at the interface between antigen-presenting cells (APCs) and T lymphocytes (Monks *et al*, 1998; Wulfing and Davis, 1998; Grakoui *et al*, 1999). During antigen presentation, the T cell relocates adhesion and activating receptors, cytoskeletal components and related organelles to the contact site with the APC. T-cell receptors (TCRs) gather at this site, and form the central supramolecular activation cluster (cSMAC), which also includes CD3 and co-stimulatory receptors. The cSMAC is surrounded by a ring of adhesion receptors that form the peripheral SMAC (pSMAC) (Dustin *et al*, 1998; Mittelbrunn *et al*, 2004). Polarization of the

*Corresponding author. Servicio de Inmunología, Planta 1, Hospital de La Princesa, Diego de León 62, Madrid, Madrid 28006, Spain.
Tel.: +34 915202370; Fax: +34 915202374;
E-mail: fsanchez.hlpr@salud.madrid.org
[6]These authors contributed equally to this work

Received: 13 September 2010; accepted: 12 January 2011; published online: 15 February 2011

cytoskeleton towards the IS involves polymerization of actin, which, together with myosin, forms a contractile ring that is important for the correct concentration of the TCR complex at the cSMAC (Gomez and Billadeau, 2008; Ilani *et al*, 2009). The tubulin cytoskeleton also reorganizes, and the microtubule-organizing centre (MTOC) is reorientated towards the IS through the activity of dynein/dynactin molecular motors (Martin-Cofreces *et al*, 2008). Under these circumstances, the cytoskeleton guides the redistribution of the secretory and Golgi apparatus towards the IS, which favours the polarized secretion and endocytic recycling of receptors at the IS (Vicente-Manzanares and Sanchez-Madrid, 2004). Mitochondria have been shown to relocate towards the IS, where their role in the maintenance of Ca_i^{2+} flux is important for T-cell activation (Quintana *et al*, 2007). However, the molecular mechanisms driving mitochondrial positioning at IS and the role of mitochondria in IS organization and TCR signalling have not been addressed.

We show here that, upon TCR triggering, the mitochondrial fission factor Drp1 docks at mitochondria and regulates relocation of mitochondria to the nascent pSMAC, where they control myosin activity and cSMAC assembly. Moreover, Drp1 controls mitochondrial depolarization and TCR signalling. Our data indicate that Drp1 is an important modulator of T-cell activation, driving mitochondrial positioning and function at the IS.

Results

T-cell activation promotes mitochondrial translocation towards the pSMAC

The precise localization of mitochondria during IS formation was assessed by confocal microscopy of Jurkat T cells conjugated with superantigen-E (SEE)-pulsed Raji cells or haemagglutinin (HA) peptide-pulsed HOM2 B cells as APCs. In both experimental systems of cell activation, most T-cell mitochondria moved in an orchestrated manner towards the IS, where the MTOC was situated (Figure 1A and B; Supplementary Figure S1). These synaptic mitochondria surrounded the central TCR/CD3 cluster and were located beneath the actin ring at the pSMAC (Figure 1C and D).

The kinetics of mitochondria translocation during IS formation was studied in human primary T lymphoblasts plated onto planar lipid bilayers containing GPI-linked ICAM-1 and anti-human CD3 antibody. CD3 microclusters appeared early at the periphery of the IS structure, and then moved centripetally to form the cSMAC (Figure 1E). Simultaneously with the redistribution of CD3 to form a central cluster, mitochondria spread near the cell–bilayer interface during the first 3 min after plating and then relocated towards the pSMAC to form a ring around the TCR/CD3 central cluster (Figure 1E and F). This mitochondrial reorganization was also analysed by total internal reflection fluorescence microscopy (TIRFM), revealing movement of mitochondria from the periphery of the contact area towards the centre of the IS (Figure 1G). Although some mitochondria appeared to move in and out of the cSMAC, most were localized at the pSMAC (see also Supplementary Movie S1). These results indicate that during the formation of the IS, mitochondria relocate to form a ring-shaped structure at the pSMAC of the IS.

Drp1 mediates mitochondrial positioning at the IS

The mitochondrial fission factor Drp1 is a key component of the mitochondrial dynamics machinery (Chang and Blackstone, 2010). Previous studies showed that dissociation of Drp1 from mitochondria occurs concomitantly with mitochondrial mislocalization (Varadi *et al*, 2004), suggesting that Drp1 may have a role in mitochondrial redistribution and positioning in highly polarized cells. We therefore studied whether, in response to antigen-pulsed APC, Drp1 associates with mitochondria in T cells and enables their translocation and positioning at the IS. Double immunofluorescence microscopy analysis showed that Drp1 localized with mitochondria at the IS of T cells conjugated with SEE- or HA-pulsed APC (Figure 2A–C). Accordingly, cell fractionation analysis confirmed recruitment of Drp1 to mitochondria in antigen-specific T cell–APC conjugates (Figure 2D and E) but not in the absence of antigen (Supplementary Figure S2). To determine whether Drp1 drives the redistribution of mitochondria towards the IS, we silenced Drp1 expression in J77 T cells using Drp1-specific siRNAs (Figure 2F) and studied the localization of their mitochondria in antigen-specific conjugates with APC. Mitochondrial translocation towards the IS was reduced in Drp1 knockdown J77 T cells stimulated with SEE-pulsed Raji B cells (Figure 2G and H). Interestingly, under these experimental conditions, MTOC translocation was unaffected (Figure 2G and I). The expression of YFP-fused wild-type Drp1 (Drp1WT-YFP) in Drp1 knockdown J77 T cells restored SEE-dependent mitochondrial translocation (Figure 2J–L), confirming that Drp1 silencing specifically interfered with this process.

The above results suggest that Drp1 regulates mitochondrial localization directly by acting on mitochondria dynamics. To assess this, we uncoupled Drp1 from mitochondria by two approaches: overexpression of a phosphomimetic S637D mutant of Drp1 (Drp1S637D-YFP) or treatment of cells with mitochondrial division inhibitor-1 (mdivi-1). These approaches prevent Drp1 docking at the mitochondrial outer membrane and consequently reduce mitochondrial fission (Cassidy-Stone *et al*, 2008; Cereghetti *et al*, 2008; Tanaka and Youle, 2008). Expression of Drp1S637D-YFP reduced SEE-induced mitochondrial redistribution compared with overexpression of Drp1WT-YFP or a non-phosphorylable Drp1 mutant (Drp1S637A-YFP) (Figure 3A and B). Similar results were obtained when T cells were treated with mdivi-1 (Figure 3C and D). Transmission electron microscopy (TEM)-based morphometric studies of T cell–APC conjugates revealed that mitochondria in mdivi-1-treated cells were farther from the IS and were enlarged in area and perimeter compared with control cells (Figure 3E and F).

Translocation of the MTOC is a prerequisite for mitochondrial redistribution to the IS in T cells, as shown by the delocalization of mitochondria when MTOC reorientation is prevented (see Supplementary Figure S3A–C). Therefore, these results indicate that, in addition to microtubules, mitochondrial translocation towards the pSMAC of the IS depends on Drp1 assembly at the mitochondrial outer membrane and subsequent mitochondrial fission.

Drp1 controls IS architecture

To determine whether Drp1-mediated mitochondrial redistribution and positioning at the pSMAC is important for IS organization, we studied the effect of Drp1 silencing

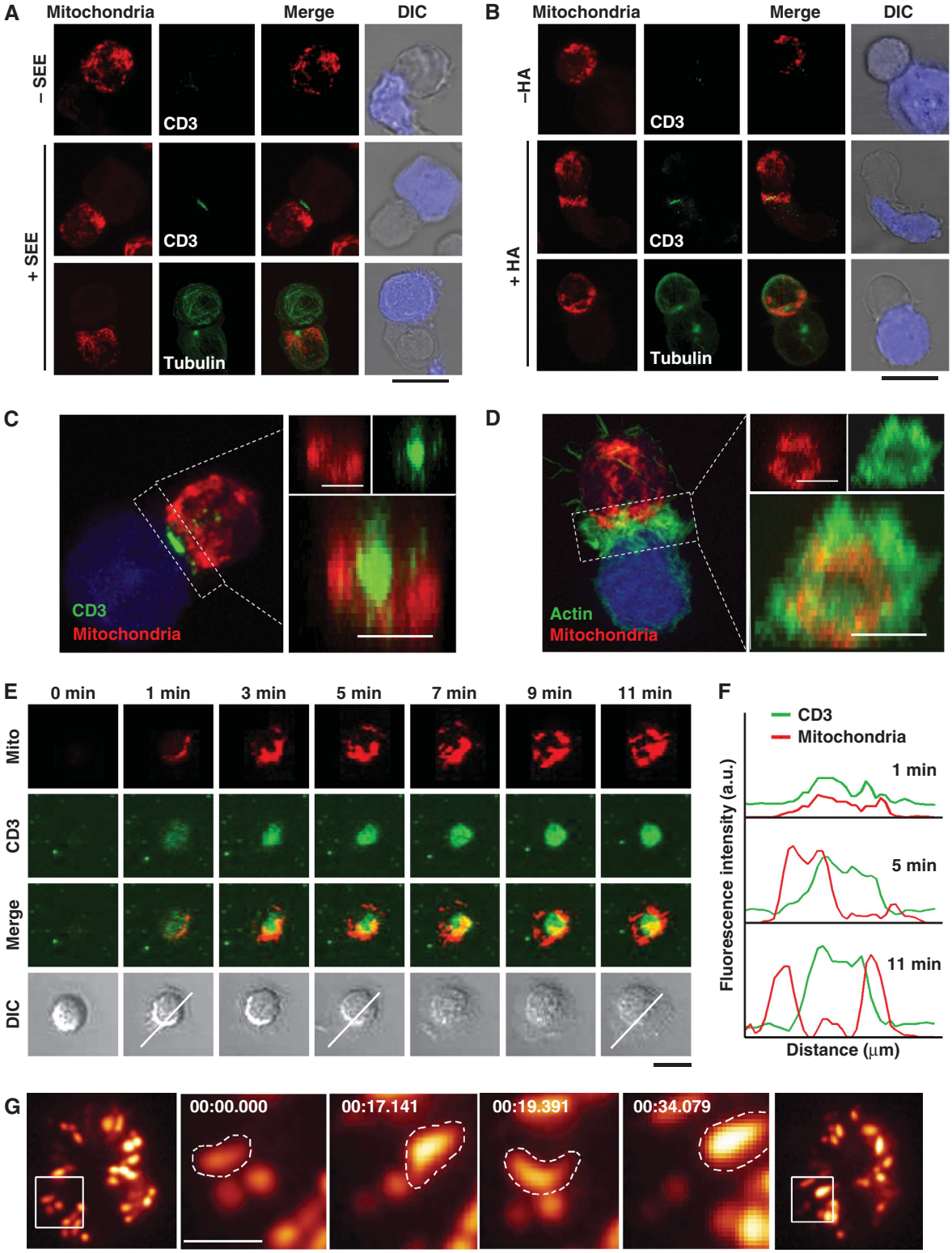

Figure 1 Mitochondria translocate towards the pSMAC upon T-cell activation. (**A**) J77 T cells loaded with Mitotracker Orange (red) were conjugated with unpulsed or SEE-pulsed Raji B cells loaded with CMAC (blue). Cells were stained with anti-CD3 or anti-tubulin-FITC (green) to reveal TCR clustering and MTOC orientation. (**B**) Analysis as in (**A**) of HA-specific CH7C17 T cells conjugated with unpulsed or HA-pulsed Hom2 APCs. Scale bars, 10 μm. (**C**, **D**) Maximum projection of a confocal *Z*-stack of conjugates stimulated as in (**A**). Cells were stained with CD3 Ab (**C**) or phalloidin (**D**) (green) to determine the areas of the cSMAC and pSMAC. Right panels show maximal projection of 3D reconstructions from the IS. Scale bars, 5 μm. (**E**) Migration of mitochondria towards the IS in mitotracker-preloaded human T lymphoblasts adhered to GPI-linked ICAM-1 and anti-CD3-containing lipid bilayers. CD3 clusters (green) and mitochondria (red) were detected by confocal microscopy at the indicated times on a single confocal plane. Scale bar, 5 μm. (**F**) Fluorescence intensity profiles from (**E**) show the pSMAC localization of mitochondria at the indicated times. (**G**) TIRF microscopy of mitoYFP expressing T cells plated on a CD3 plus CD28 Ab surface. Magnified views show forward–backward movement of a mitochondrion at the edge of the contact with the activating surface. Scale bar, 1 μm.

on CD3 assembly at the cSMAC. Although Drp1 knockdown did not alter the expression levels of CD3 or LFA-1 on the plasma membrane of J77 T cells (data not shown), the central clustering of TCR/CD3 at the IS was inhibited (Figure 4A and B). 3D reconstruction of the IS formed by Drp1-silenced J77 cells and SEE-pulsed APCs revealed a scattered distribution of CD3 (Figure 4C and D), an enlarged cSMAC diameter (Figure 4E) and an increased number of CD3 microclusters (Figure 4F). Consistently, in planar lipid bilayer assays, Drp1-silenced cells did not form a cSMAC, and CD3 microclusters were unable to coalesce at the centre of the IS. In these cells, in contrast to control cells, mitochondria did not relocate to the IS and did not form a ring-shaped structure around the cSMAC (Figure 4G and H). These results indicate that Drp1 has an important role in the formation of the IS, linking mitochondrial positioning to the molecular organization of CD3 at the cSMAC.

Drp1 controls mitochondrial depolarization and myosin fuelling at the IS

To explore the mechanism by which Drp1-mediated mitochondrial redistribution regulates cSMAC assembly, we assessed mitochondrial function and energy status in activated T cells. We first monitored mitochondrial membrane potential ($\Delta\psi_m$) by timelapse confocal microscopy of J77 T cells expressing MitoYFP and labelled with the potentiometric dye tetramethylrhodamine methyl ester (TMRM). When these cells were plated onto CD3/CD28 Ab activating surfaces, the mitochondria closest to the bottom surface abruptly depolarized as indicated by the drop in TMRM fluorescence, whereas plating onto poly-L-lysine (PLL) plus control Ab had no effect (Figure 5A; Supplementary Figure S4). These results were confirmed by flow cytometry of whole-cell populations labelled with the mitochondria-specific cation tracker JC-1. The JC-1 emission maximum at high $\Delta\psi_m$ is 590 nm (red, detected in FL2) and shifts to 520 nm (green, detected in FL1) as $\Delta\psi_m$ decreases (Solaini *et al*, 2007). Using this label, we found that CD3/CD28 engagement diminished $\Delta\psi_m$ in human primary T lymphoblasts (Figure 5B and C). Mitochondrial depolarization was significantly enhanced in Drp1-silenced cells, even in the absence of stimulation (Figure 5B and C). We next assessed the effect of CD3/CD28 engagement on T lymphoblast intracellular ATP levels. ATP content increased in activated T cells with respect to untreated cells, an effect reverted by the mitochondrial ATP-synthase inhibitor oligomycin (Figure 6A). In contrast, CD3/CD28 stimulation did not significantly change ATP levels in Drp1-interfered cells (Figure 6A). Mitochondrial membrane potential and ATP production are thus compromised in Drp1-silenced T cells during activation, suggesting a role for Drp1 in the regulation of IS organization through the control of mitochondrial function.

To test this possibility, T cells were treated with the mitochondrial uncoupling agent FCCP (which abolishes ψ_m; Figure 6B), the ATP-synthase inhibitor oligomycin, or the mitochondrial fission inhibitor mdivi-1. Treatment of SEE-specific T cell–APC conjugates with any of these agents inhibited clustering of CD3 at the IS to a similar extent as Drp1 silencing (Figure 6C and D), thus linking Drp1-dependent mitochondrial function and depolarization to IS organization. Consistent with these results, myosin activation, an ATP-dependent process involved in IS formation (Ilani *et al*, 2009), was impaired in Drp1-silenced T lymphoblasts and J77 cells, which showed lower levels of myosin regulatory light chain (MLC) phosphorylation at Ser19 than control cells (Figure 6E). MLC phosphorylation in SEE-specific T cell–APC conjugates mostly took place at the IS of control T cells, and was strongly reduced by Drp1 silencing (Figure 6F). Given that phosphorylation of MLC at Ser19 increases the motor activity of myosin (Huttenlocher *et al*, 1995), and that myosin IIA localizes at the IS of T cells (Huttenlocher *et al*, 1995; Ilani *et al*, 2009), our results strongly suggest that ATP-dependent myosin contractile activity is diminished at the IS of Drp1-silenced T cells. Together, these results support that Drp1 regulates mitochondrial-dependent myosin fuelling at the IS by impeding persistent mitochondrial depolarization and thereby favouring ATP synthesis.

Drp1 modulates TCR signal strength

We next assessed the role of Drp1 in TCR/CD3 signalling. Microclusters of tyrosine-phosphorylated proteins were peripherally distributed in the IS of Drp1-silenced T cell–APC conjugates, contrasting with their concentration at the cSMAC in control conjugates (Figure 7A). Drp1 silencing provoked dispersal of the phospho-ERK signal at the SEE-dependent IS (Figure 7B) and a longer-lasting phosphorylation of ERK1/2 and PLC-γ1 in SEE-stimulated primary T lymphoblasts and J77 T cells (Figure 7C and D). Moreover, Ca_i^{2+} flux was also maintained for longer in Drp1-silenced J77 T cells, both upon conjugation with SEE-pulsed Raji APCs and activation with CD3 Abs (Figure 7E; Supplementary Figure S5). Finally, Drp1 silencing increased the secretion of IL-2 in SEE-dependent T cell–APC conjugates (Figure 7F). These results suggest that Drp1 modulates TCR proximal signalling and IL-2 production through the control of mitochondria positioning and activity at the IS.

Discussion

The findings presented here provide evidence that the mitochondrial fission protein Drp1 modulates T-cell activation at the IS. During T-cell–APC cognate interactions, Drp1 translocates to mitochondria and controls their positioning at the pSMAC of T cells, and thus provides a means of studying the role of mitochondria located beneath the IS. siRNA targeting or mitochondrial uncoupling of Drp1 impairs CD3 clustering at the cSMAC, thereby increasing several markers of intracellular signalling induced through the TCR upon antigen-specific activation, including activation of PLC-γ1 and ERK 1/2, intracellular Ca^{2+} flux and synthesis of IL-2 upon antigen-specific activation.

Mitochondrial trafficking and positioning have been previously described in neuronal synapses; for example, disruption of Drp1 blocks axonal transport of mitochondria in *Drosophila* and mouse brain (Verstreken *et al*, 2005; Ishihara *et al*, 2009). Our findings indicate that mitochondrial recruitment to the T-cell IS is impaired by blockade of Drp1 action, whether by siRNA silencing, treatment with the Drp1 inhibitor mdivi-1 (Cassidy-Stone *et al*, 2008; Cereghetti *et al*, 2008) or overexpression of a phosphomimetic S637D Drp1 mutant unable to bind to the OMM (Cassidy-Stone *et al*, 2008;

Cereghetti *et al*, 2008). Drp1-dependent mitochondria redistribution is required for both the proper organization of the IS and the regulation of the intracellular signalling pathways generated through the TCR. These results agree with observations in neurons, where proper distribution of mitochondria at dendritic spines and synapses is essential for neural function (Li *et al*, 2004).

Our finding that reduced cSMAC assembly of CD3 in Drp1-silenced T cells is associated with increased activation of TCR proximal elements suggests that, by controlling cSMAC orga-

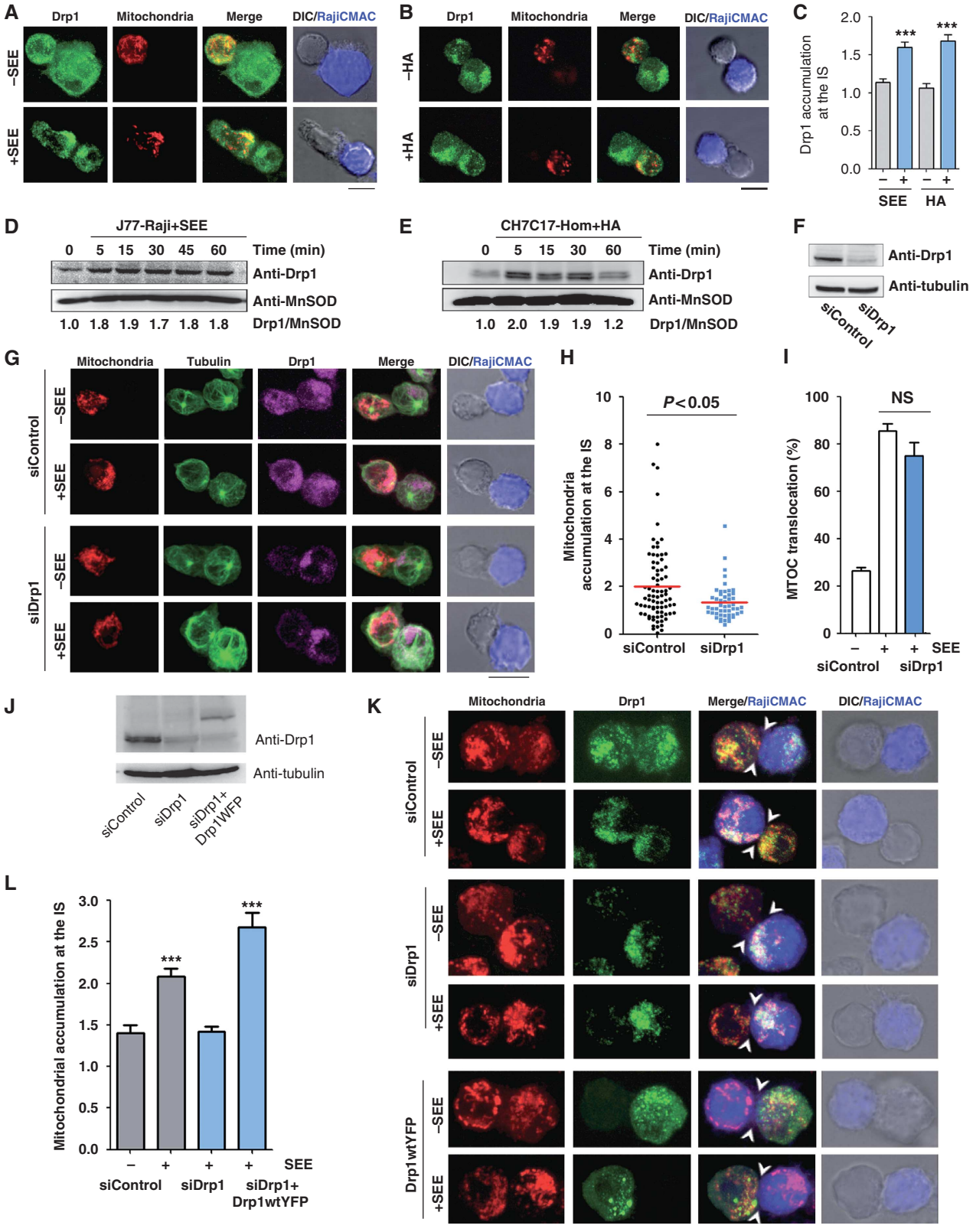

nization, Drp1 modulates T-cell activation and function. Our data moreover underscore the importance of mitochondrial positioning for fuelling molecular motors involved in IS formation, such as myosins. Myosin IIA is concentrated at the IS, from where it is suggested to control actin flux at the actomyosin contractile ring formed beneath pSMAC (Ilani *et al*, 2009). The contractility of this ring is regulated by phosphorylation of MLC and is important for directing TCR/CD3 microclusters to the cSMAC. TCR activation is initiated in the early assembled peripheral microclusters of TCR/CD3 complexes, and downmodulated in the cSMAC, where activated TCR/CD3 signalling complexes are switched off after ubiquitination, triggering their internalization and degradation by CD2AP and members of the Cbl ubiquitin ligase and

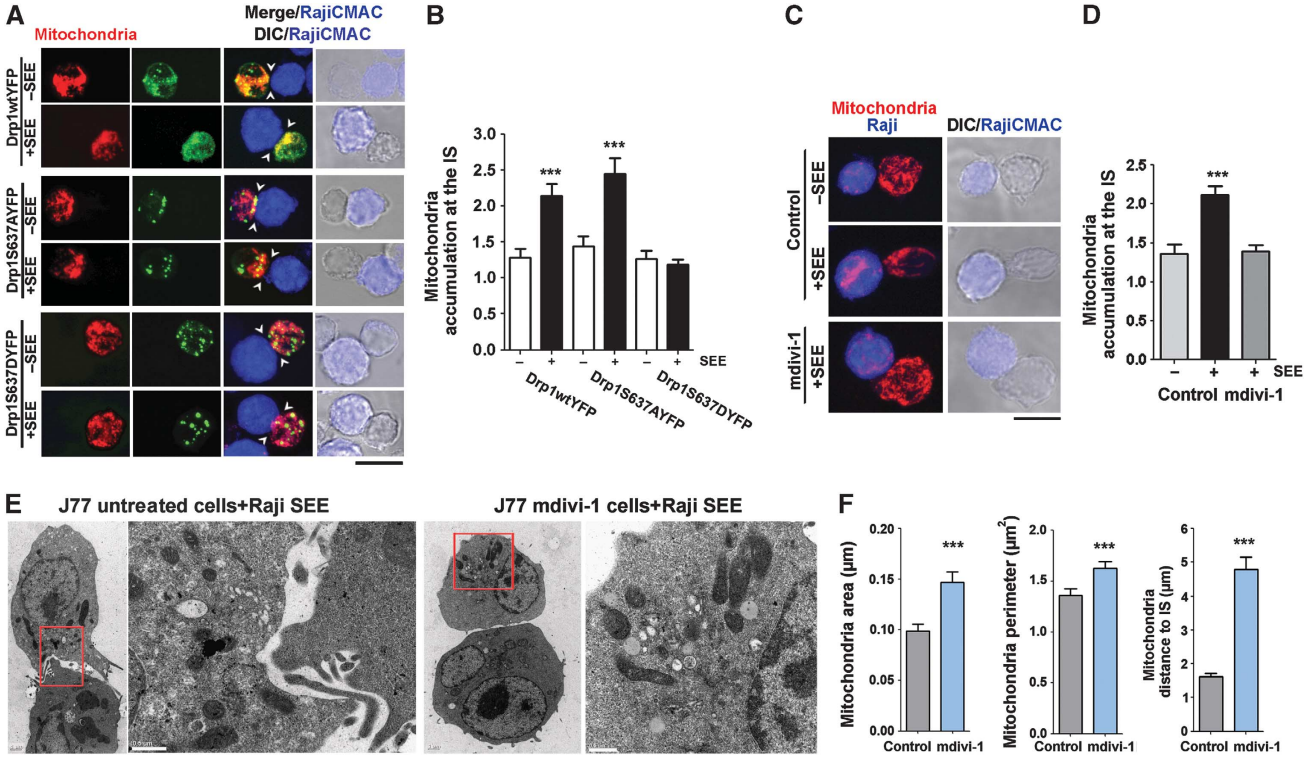

Figure 3 Drp1-mediated mitochondrial fission regulates translocation of mitochondria towards the IS. (**A**) Confocal localization of mitochondria in J77 T cells co-transfected with mtRFP (red) plus Drp1WT-YFP, Drp1S637AYFP or Drp1S637DYFP (green), and conjugated with unpulsed or SEE-pulsed Raji B cells (CMAC loaded, blue). Arrowheads mark cell–cell contacts. Scale bar, 10 μm. (**B**) Quantification of mitochondria accumulation at the IS in J77 T cells expressing Drp1WT-YFP (215 conjugates), Drp1S637AYFP (168 conjugates) and Drp1S637DYFP (141 conjugates). Data are means ± s.d. from three independent experiments (***$P<0.001$). (**C**) Confocal localization of mitochondria (MnSOD, red) in J77 cells treated with DMSO (control) or mdivi-1 (50 μM, 4 h at 37°C) and conjugated with unpulsed or SEE-pulsed Raji B cells (CMAC loaded, blue). Scale bar, 10 μm. (**D**) Quantification of mitochondria accumulation at the IS in J77 T cells conjugated as in (**C**) (248 control conjugates and 100 mdivi-1-treated conjugates). Data are means ± s.d. from two independent experiments (***$P<0.001$). (**E**) Transmission electron microscopy images from control or mdivi-1-treated J77 cells conjugated with SEE-loaded Raji B cells. Right panels show magnified views of mitochondria in the boxed areas. (**F**) Graphs showing distance of mitochondria to the IS and morphometric analysis of mitochondria area and perimeter. T-cell mitochondria were analysed in 10 SEE-dependent conjugates formed by control J77 T cells (109 mitochondria) and seven SEE-dependent conjugates formed by mdivi-1-treated J77 T cells (89 mitochondria) (***$P<0.05$).

Figure 2 Drp1 regulates mitochondrial positioning at the IS. (**A**, **B**) Immunofluorescence localization of Drp1 (green) in mitotracker-loaded T cells (red) conjugated with unpulsed or antigen-loaded APCs (CMAC loaded, blue): (**A**) J77 T cells plus SEE-pulsed Raji B cells; (**B**) CH7C17 T cells plus HA-pulsed Hom2 cells. (**C**) Endogenous accumulation of Drp1 at the IS in J77 T cells conjugated with unpulsed or SEE-pulsed Raji B cells or CH7C17 T cells conjugated with naive or HA-pulsed Hom2 APCs. Maximum projections of a confocal *Z*-stack were quantified (see Materials and methods). Data are means ± s.d. of 60 conjugates from two independent experiments. (**D**, **E**) Time course of Drp1 content in the mitochondrial fractions of APC-activated J77 and CH7C17 T cells. MnSOD was used as mitochondrial marker. Blots are representative of at least three independent experiments. Drp1/MnSOD ratios are shown beneath the blot. (**F**) Western blot analysis of siRNA Drp1 silencing in J77 T cells after 48 h. (**G**) Confocal localization of mitochondria (mitotracker, red), MTOC (tubulin, green) and endogenous Drp1 (purple) in control and Drp1-silenced J77 T cells conjugated with Raji B cells (CMAC loaded, blue). Scale bar, 10 μm. (**H**, **I**) Quantification of mitochondrial accumulation and MTOC positioning at the IS in Drp1-silenced cells. Data in (**H**) represent means ± s.d. of 60 conjugates from three experiments ($P<0.05$, Mann–Whitney test). (**J**) Western blot analysis of siRNA Drp1 silencing in J77 T cells and re-expression of YFP-fused wild-type Drp1 (Drp1WT-YFP). (**K**) Confocal localization of mitochondria (labelled with anti-MnSOD, red) and endogenous Drp1 (green) in control and Drp1-silenced J77 T cells conjugated with Raji B cells (CMAC loaded, blue) as in (**G**). Re-expression Drp1WT-YFP (green) in Drp1-silenced cells rescues mitochondrial translocation towards the IS upon conjugation with SEE-pulsed Raji B cells (CMAC loaded, blue). Arrowheads mark cell–cell contacts. Scale bar, 10 μm. (**L**) Accumulation of T-cell mitochondria at the IS of conjugates formed between Raji B cells and J77 T cells expressing control siRNA (88 −SEE conjugates and 231 +SEE conjugates), Drp1-siRNA (148 conjugates), and Drp1-siRNA plus Drp1WT-YFP (78 conjugates). Data are means ± s.d. from two independent experiments (***$P<0.001$).

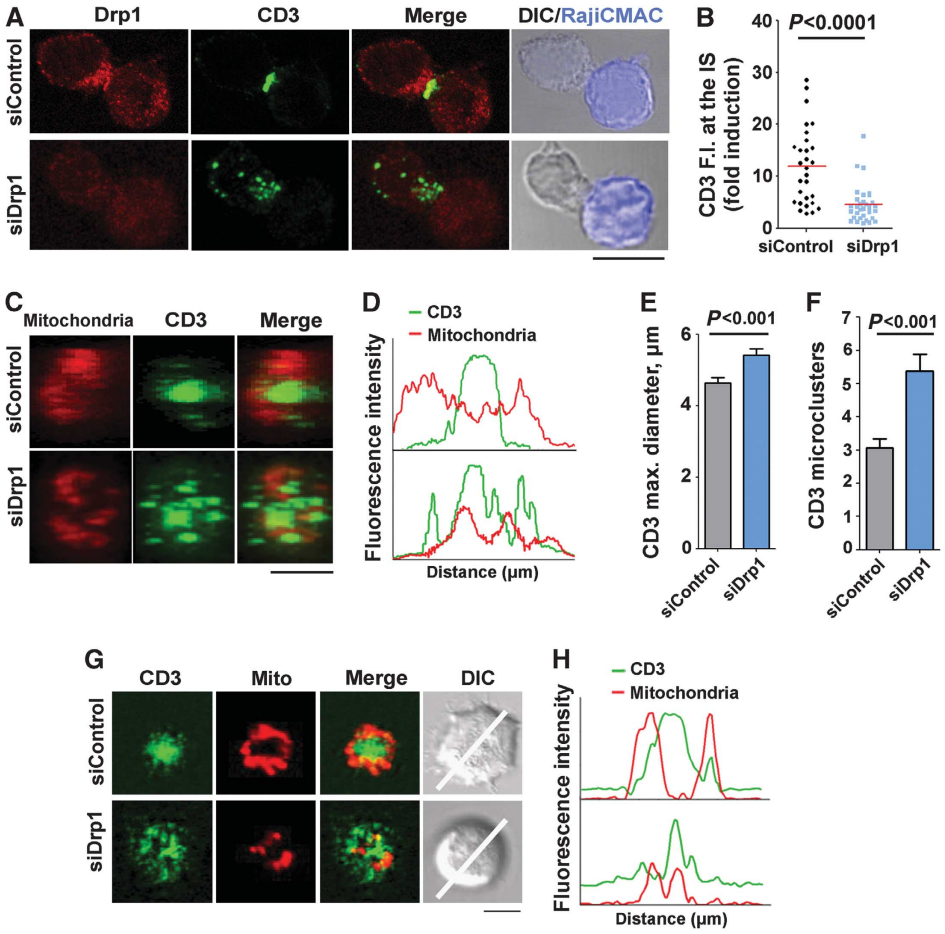

Figure 4 Drp1 controls IS organization. (**A**) Distribution of Drp1 (red) and CD3 (green) in conjugates between control or Drp1-silenced J77 T cells and SEE-pulsed Raji B cells (CMAC loaded, blue). Scale bar, 10 μm (**B**) Quantification of CD3 accumulation at the IS, calculated from maximal confocal *Z*-projections in 30 cells from two independent experiments ($P<0.0001$, Mann–Whitney test) (**C**) 3D reconstructions of the cell–cell contact area in control and Drp1-silenced J77-APC conjugates; note the dispersed organization of the CD3/TCR in Drp1-silenced cells. Scale bar, 5 μm (**D**) Profile plot of the staining intensities of CD3 (green) and mitochondria (red) in the structures depicted in (**C**). (**E**, **F**) CD3 diameter ($P<0.001$ in Student's *t*-test; 58 conjugates) and CD3 cluster number ($P<0.001$, Mann–Whitney test; 50 conjugates) calculated from 3D reconstructions of T cell–APC contacts. Data are means ± s.d. from three independent experiments. (**G**) Confocal analysis of IS structures formed in mitotracker-loaded control or Drp1-silenced J77 cells (red) adhered for 20 min to lipid bilayers containing anti-CD3 (green) and GPI-ICAM-1. A representative cell from one experiment of three is shown. Scale bar, 5 μm. (**H**) Profile plots of fluorescence intensities for CD3 and mitochondria along the lines indicated in (**G**).

ESCRT (endosomal sorting complex required for transport) families (Lee *et al*, 2003; Malissen, 2003; Varma *et al*, 2006; Vardhana *et al*, 2010). Silencing of myosin IIA prevents the formation of the cSMAC and the amplification of TCR signals (Ilani *et al*, 2009). Accordingly, our data show that Drp1 silencing reduces MLC phosphorylation at Ser19, elevates the number of CD3 microclusters and disrupts TCR/CD3 complex organization at the cSMAC. A similar effect on MLC phosphorylation has been described for Drp1 mutants during the mobilization of pool vesicles at *Drosophila* neuromuscular junctions (Verstreken *et al*, 2005). Our findings provide a plausible explanation of how mitochondrial delocalization from the IS might disturb cSMAC formation and subsequent signalling. By reducing actomyosin fuelling at the IS, mitochondrial delocalization in Drp1-interfered T cells slows centripetal flux of TCR/CD3 microclusters, thus enhancing signalling by maintaining TCR/CD3 complexes away from cSMAC-localized degradation pathways.

The enhanced mitochondrial membrane depolarization in Drp1-silenced cells suggests that Drp1 regulates the extent of mitochondrial membrane depolarization. Enhanced mitochondrial depolarization prevents both the clustering of the TCR/CD3 at the cSMAC and the cessation of TCR-dependent signalling, resulting in persistent T-cell activation, intracellular Ca^{2+} flux and diminished ATP synthesis. Our results showing that Drp1 silencing increases mitochondrial depolarization in stimulated and non-stimulated T cells argue for a direct role of Drp1 in controlling mitochondrial function during T-cell activation. Mitochondria located at sites of T-cell stimulation control local Ca^{2+} influx (Schwindling *et al*, 2010), and our results therefore support a role for Drp1-mediated mitochondrial positioning in the buffering of Ca^{2+} at the IS. The IS is the main entry point for Ca^{2+} upon TCR stimulation (Schwindling *et al*, 2010), which suggests that Drp1 impedes intramitochondrial diffusion of Ca^{2+} during TCR signalling by maintaining the compartmentalization of the mitochondrial network at the IS through fission events. In this regard, our results support the idea that T cells fine-tune TCR responses through Drp1-mediated regulation of mitochondrial positioning and activity. Furthermore, mitochondria positioning at the IS is essential for the management of intracellular Ca^{2+} levels, and

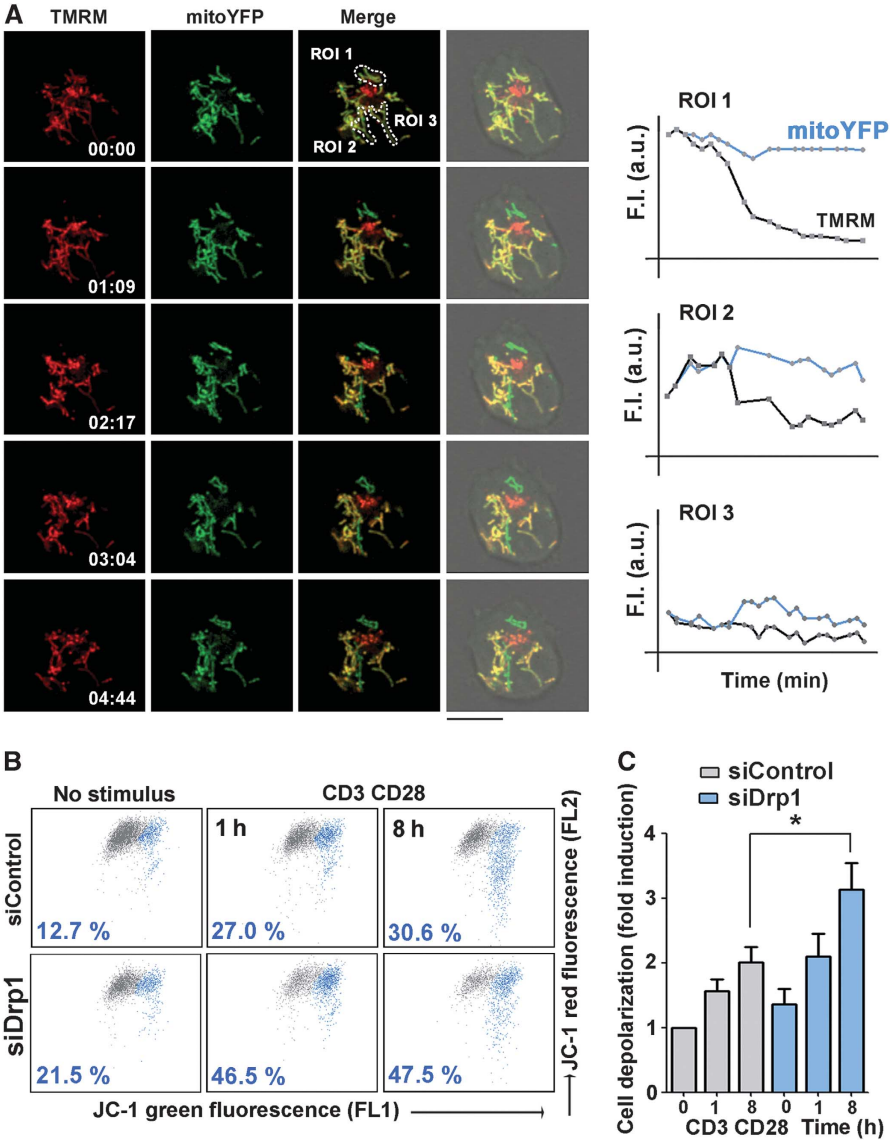

Figure 5 Mitochondria depolarize at sites of TCR activation. (**A**) Confocal video-microscopy of mitoYFP-transfected J77 T cells loaded with the mitochondrial membrane potential dye TMRM and plated on coverslips coated with CD3 plus CD28 Abs. Images record the movement of individual mitochondria in a confocal plane at the activating surface. Profile plots show time courses of mitoYFP and TMRM fluorescence intensity in the indicated mitochondria (regions of interest, ROI), showing variations in $\Delta\psi_m$ (see Materials and methods section). (**B**, **C**) Flow cytometry analysis of mitochondrial membrane potential ($\Delta\psi_m$ FL2 versus FL1 JC-1 fluorescence) in control and Drp1-silenced human T lymphoblasts activated with anti-CD3 (10 μg/ml) plus anti-CD28 (5 μg/ml) and loaded with the mitochondrial potentiometric tracker JC-1. (**B**) The dot plots show a representative experiment of four. The percentage cell population with depolarized mitochondria (blue) is indicated. (**C**) Quantification of cells exhibiting mitochondrial depolarization in control and siDrp1-expressing human T lymphoblasts activated with CD3 plus CD28 Abs. Data are means ± s.d. from four donors ($^*P<0.05$).

Drp1-dependent fragmentation of the mitochondrial network may serve to protect T cells from amplified calcium signalling triggered by activation.

The actin-rich area of the pSMAC is highly homologous with the actin-rich areas at neuronal postsynaptic termini. These actin-rich, membrane receptor-driven structures serve as scaffolds for selective and profuse secretion, and our finding that mitochondria dock at the actin-rich pSMAC area of the IS suggests that similar mechanisms operate in T cells. Whereas actin is involved in mitochondrial docking at neuronal synapses (Hollenbeck and Saxton, 2005; MacAskill and Kittler, 2010), mitochondrial trafficking is dependent on microtubules and members of the microtubule-associated kinesin and dynein motor-protein families. Mutations in dynein heavy chain or p150GLUED block axonal mitochondrial trafficking, affecting both anterograde and retrograde transport (Martin *et al*, 1999; Pilling *et al*, 2006). Dynein/dynactin motor complexes are important for T-cell activation, preventing MTOC translocation and the formation of the CD3/TCR central cluster at the IS (Martin-Cofreces *et al*, 2008). In this regard, we also observed a defect in mitochondria relocalization at the IS when dynein/dynactin motor activity is inhibited. Nevertheless, our results demonstrate that Drp1-mediated mitochondrial transport towards the IS also requires assembly of Drp1 at the mitochondrial outer membrane and consequent mitochondrial fission, therefore suggesting that mitochondrial transport towards the IS may require interaction between Drp1 and dynein. How Drp1-

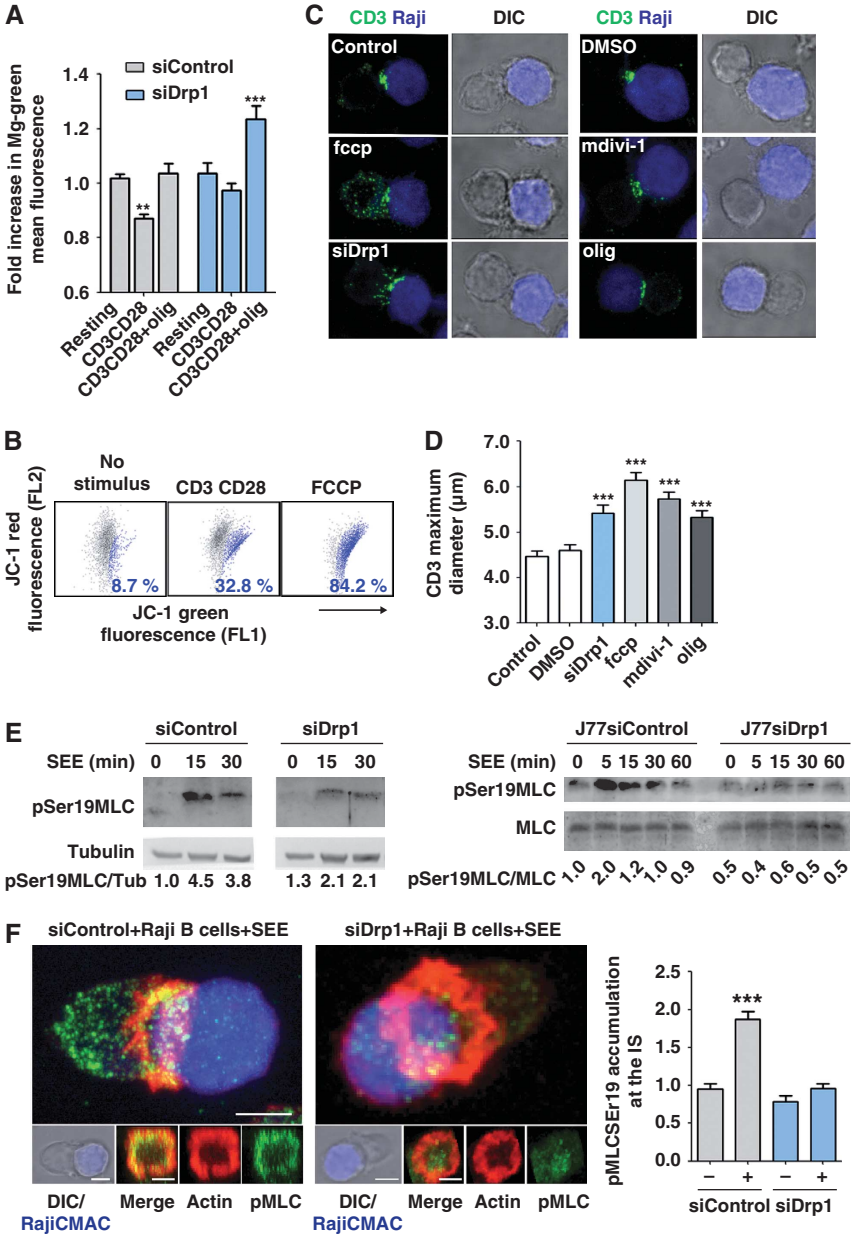

Figure 6 Drp1 regulates T-cell activation-induced mitochondrial depolarization and myosin fuelling at the IS. (**A**) Relative ATP content was measured with the magnesium green probe (Mg-Gr), whose fluorescence intensity inversely correlates with intracellular ATP. Control and Drp1-silenced J77 T cells were stimulated with CD3 plus CD28 Abs and treated with vehicle or oligomycin. Data are means ± s.d. from three independent experiments performed in triplicate (**$P<0.01$, ***$P<0.001$). (**B**) Dot plots of FL1 and FL2 JC-1 fluorescence in human T lymphoblasts activated with CD3 plus CD28 Abs and loaded with JC-1 as in Figure 5B. FCCP (250 nM) was used for maximal $\Delta\psi_m$ depolarization. A representative experiment is shown with primary T lymphoblasts from one of the three donors. (**C**) Confocal analysis of CD3 organization (green) in SEE-dependent conjugates formed by control J77 T cells, Drp1-silenced J77 T cells or J77 cells treated with mdivi-1, FCCP, oligomycin or vehicle. SEE-pulsed Raji B cells were CMAC loaded (blue). Scale bar, 10 µm. (**D**) CD3 maximum diameter in J77 T cells conjugated as in (**C**). The numbers of conjugates analysed for each condition were 409 (control), 136 (siDrp1), 313 (midiv-1), 339 (FCCP) and 230 (oligomycin). Data are means ± s.d. from three independent experiments (***$P<0.001$). (**E**) Time course of the phosphorylation of myosin regulatory light chain at Ser19 in conjugates formed between control and Drp1-silenced human primary T lymphoblasts or J77 T cells and SEE-pulsed Raji B cells. Total expression of MLC and tubulin are shown as loading controls. Representative blots of three experiments are shown. Numbers beneath the blots denote pMLC/Tub and pMLC/MLC ratios. (**F**) Confocal analysis of pMLCSer19 (green), actin (red) in control and siDrp1 J77 T cells conjugated with SEE-pulsed Raji B cells (CMAC, blue). 3D stack reconstructions show pMLCSer19 and the actin ring at the contact site between control and siRNA Drp1-silenced J77 T cells and the APC. The chart shows quantification of pMLCSer19 accumulation at the IS in control and siDrp1-silenced cells in SEE-specific conjugates. Data are means ± s.d. from two independent experiments (***$P<0.001$).

mediated mitochondrial fission facilitates transport remains unclear. It is feasible that binding to mitochondria exposes the dynein-binding site on Drp1 or that dynein more efficiently traffics fragmented mitochondria than an extensively fused mitochondrial meshwork. This would imply that dynein-dependent trafficking coordinates MTOC movement with mitochondrial activity for the local delivery of biological mediators at the IS, similar to the relationship observed between the MTOC and the T-cell secretory machinery (Kupfer and Singer, 1989; Huse *et al*, 2006). MTOC transloca-

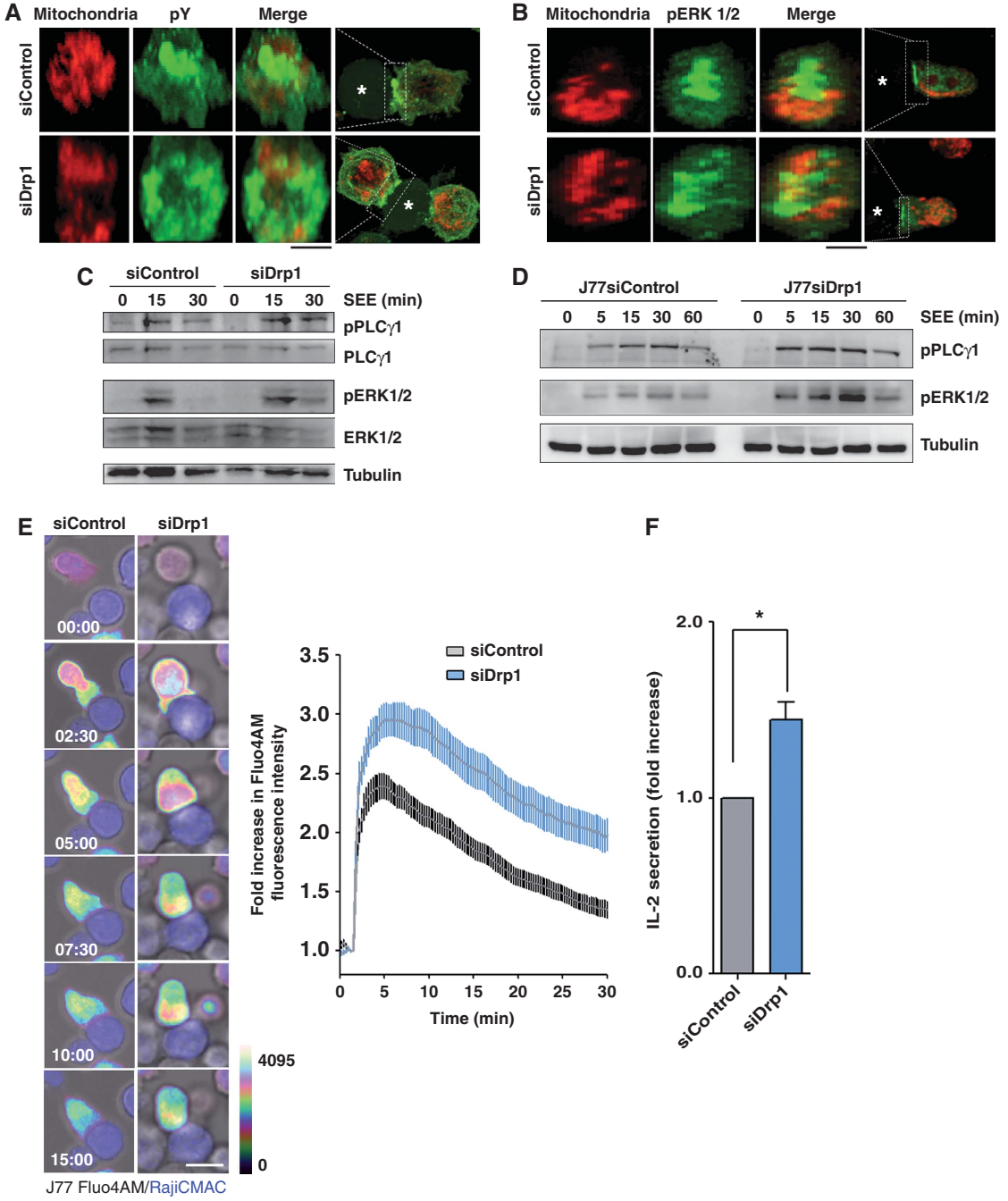

Figure 7 Drp1 regulates TCR signal strength. (**A**, **B**) Confocal 3D stack reconstructions showing the distribution of phosphotyrosine (pY) (**A**) and phosphorylated ERK1/2 (**B**) at the contact site between mitotracker-loaded control or Drp1-silenced J77 T cells and SEE-pulsed Raji B cells (asterisks). (**C**, **D**) Time course of the phosphorylation status of PLC-γ1 and ERK 1/2 in control and Drp1-silenced human primary T lymphoblasts (**C**) or J77 T cells (**D**) activated with SEE-pulsed Raji B cells. Tubulin or total protein expression are shown as loading controls. Immunoblots are representative of three independent experiments. (**E**) Confocal microscopy analysis of intracellular Ca^{2+} flux in control and Drp1-silenced J77 T cells preloaded with Fluo4 AM and conjugated with SEE-pulsed Raji B cells (CMAC, blue). The time profile shows the evolution of Fluo4 AM fluorescence in control (56 conjugates) and siDrp1 (86 conjugates) conjugates. Data are means ± s.d. from three independent experiments ($P<0.0001$, two-tailed *t*-test). (**F**) IL-2 secretion from conjugates formed between SEE-pulsed Raji cells and control or Drp1-silenced J77 cells. IL-2 was measured by ELISA 16 h after initial conjugate formation. Data are means ± s.d. of six independent experiments ($^*P<0.05$).

tion is unaffected by Drp1 silencing, providing further evidence that dynein/dynactin transports not only the MTOC but also mitochondria towards the IS, through coordinated action with Drp1. However, it remains possible that other molecular motors such as kinesins also have a role in directing mitochondria towards the IS.

The finding that mitochondrial fission factors are involved in IS formation and T-cell function further emphasizes the commonalities between the immune and neural systems. Understanding of neuronal and immune synapse function might therefore be effectively advanced by deciphering shared mechanisms that target and regulate mitochondria

to both types of synapse. Further work is needed to address the relation between mitochondrial dynamics and transport machineries, to determine how mitochondria are anchored to the IS and to identify the signals that relocate mitochondria to sites of high demand for energy and Ca^{2+} buffering. It will also be of great interest to investigate the link between the mitochondrial fission machinery and T-cell survival and differentiation, in order to define the role of mitochondrial network dynamics and activity in the adaptive immune response.

Materials and methods

Reagents and antibodies

Fibronectin (FN), PLL, TMRM, 5,5′,6,6′-tetrachloro-1,1′,3,3′-tetraethylbenzimidazolcarbocyanine iodide (JC-1), carbonyl cyanide 4-(trifluoromethoxy)phenylhydrazone (FCCP), RU360, influenza HA peptide, and FITC-conjugated or unconjugated anti-α-tubulin and anti-γ-tubulin were from Sigma-Aldrich (St Louis, MO). *Staphylococcus enterotoxin* E was from Toxin Technology (Sarasota, FL). Alexa 488 and 647, phalloidin 488, cell tracker 7-amino-4-chloromethylcoumarin (CMAC), INDO-1, Fluo4-AM and Mitotracker Orange were from Invitrogen (Carlsbad, CA). The antibody T3b (anti-human-CD3) was produced in our laboratory. Erk1/2 and p74-dynein Abs were from Millipore (Billerica, MA); phospho-Erk1/2, phospho-PLC-γ1 (Y783), PLC-γ1 Ab from Cell Signaling Technology (Denver, MA); monoclonal Drp1 Ab from BD Transduction Laboratories (Lexington, KY); polyclonal Drp1, phospho-specific Ser19 MLC and MLC2 Abs from Santa Cruz Biotechnology (Santa Cruz, CA); and MnSOD Ab from Rockland (Gilberstsville, PA).

Cells, plasmids and cell transfection

Human T lymphoblasts were obtained from human peripheral blood lymphocytes by treatment for 48 h with 1 μg/ml PHA, followed by 50 U/ml IL-2 in complete RPMI 1640 medium until day 11. SEE-specific human T lymphoblasts were obtained as described (Ibiza *et al*, 2006). Vβ8+ Jurkat T-cell clones (J77) and the lymphoblastoid Raji and Hom2 B cell lines were cultured in complete medium. HA-specific, Vβ3+ Jurkat T cells (CH7C17) were supplemented with 400 μg/ml hygromycin B and 4 μg/ml puromycin. Plasmids encoding mtRFP, mtYFP, Drp1wtYFP, Drp1S647AYFP, Drp1S647DYFP were as previously described (Cereghetti *et al*, 2008), and generously provided by Dr L Scorrano (University of Geneva, Switzerland). T-cell lines and human T lymphoblasts were transfected with DNA plasmids or with specific Drp1 double-stranded siRNAs against human Drp1 (GGUGCCUGUAGGUGAU CAA) or negative control (Eurogentec) using the Gene Pulser II electroporation system (Bio-Rad Laboratories) or the Nucleofector system (Amaxa Biosystems, Gaithersburg, MD).

T-cell activation, mitochondrial isolation and immunoblotting

For TCR stimulation, cells were left untreated or treated with T3b antibody (10 μg/ml) plus cross-linker (IgG, 5 μg/ml), with or without additional CD28 Ab (5 μg/ml) for co-stimulation. For antigenic stimulation, Raji cells were pulsed with 1 μg/ml SEE (20 min) and mixed with Jurkat cells or SEE-specific human T lymphoblasts (30 min); alternatively, Hom2 cells pulsed with 200 μg/ml HA peptide (3 h) were mixed with CH7C17 cells. Cells were lysed in 50 mM Tris–HCl, pH 7.5, containing 1% NP40, 0.2% Triton X-100, 150 mM NaCl, and phosphatase and protease inhibitors. For mitochondrial fractionation, cells were lysed in ice-cold isotonic sucrose buffer (10 mM Tris pH 7.5, 0.25 M sucrose, 0.1 mM EDTA) containing protease and phosphatase inhibitors (Roche, Basel, Switzerland). Cells were then homogenized using a 23G needle. Lysates were spun at 1000 *g* (4°C, 10 min) to remove debris and nuclei, and the supernatant was further centrifuged at 13 000 *g* (4°C, 30 min) to yield the mitochondrial fraction. Mitochondrial enriched fractions were washed and proteins were resolved by SDS–PAGE and transferred to nitrocellulose membranes. After blocking, membranes were blotted with primary and peroxidase-labelled secondary antibodies and detected with western reagents (GE Healthcare, UK) and the LAS-3000 chemiluminiscent system (Fujifilm).

Cell conjugate formation, IS analysis and IL-2 production

Raji B cells or Hom2 B cells were loaded with the CMAC tracker and incubated with SEE or HA peptide. T cells (1×10^5 cells) were mixed with APC (1:1), centrifuged at low speed to favour conjugate formation, gently resuspended, and plated onto PLL-coated slides. Cells were allowed to settle for 30 min at 37°C, fixed with 4% paraformaldehyde in PBS, and permeabilized with 0.2% Triton X-100 in TBS for 5 min. Cells were processed for immunofluorescence, and mounted in Prolong antifade medium (Invitrogen). To measure the maximum diameter of CD3 clusters, J77 T cells were preincubated at 37°C, 4 h with 200 nM FCCP (Fluka, Germany), 50 μM mdivi-1, 4 μM oligomycin or DMSO (Sigma-Aldrich), and then incubated 30 min with SEE-pulsed or unpulsed CMAC-loaded Raji B cells. CD3 maximum diameter was quantified in three independent experiments using ImageJ software.

CD3 organization at the IS was analysed in APC-conjugated control and Drp1-silenced T cells. 3D *Z*-stacks of the cell–cell contact area were reconstructed, and maximum diameter and the number of CD3 clusters were quantified in 15–20 conjugates in at least three independent experiments.

CD3, mitochondria, Drp1 and pMLC accumulation at the IS was quantified in J77 or CH7C17 T cells conjugated with antigen-pulsed or non-pulsed Raji or Hom2 cells loaded with CMAC. For quantification in individual ISs, we used a home-made plugin for Image J software (http://rsbweb.nih.gov/ij/) called '*Synapse Measures*'. By comparing fluorescence signals from multiple regions of the T cell, APC, IS, and background fluorescence, the program yields accurate measurements of localized immunofluorescence. A detailed description of *Synapse Measures*, including the algorithms used, is described (Calabia-Linares *et al*, 2011).

The proportion of conjugates showing redistribution of the T-cell MTOC close to the APC contact area was determined as described (Ibiza *et al*, 2006).

Mitochondrial accumulation at the IS was calculated as the ratio of the FI of T-cell mitochondria located in the third of the cell near the APC contact area to the FI of the mitochondria in the rest of the cell. IL-2 secretion was detected by ELISA as described (Martin-Cofreces *et al*, 2008).

Timelapse fluorescence confocal microscopy and TIRFM

Raji APCs (5×10^5; SEE-pulsed or unpulsed) were allowed to adhere to FN-coated coverslips in Attofluor open chambers (Invitrogen) at 37°C in a 5% CO_2 atmosphere. T cells were added (1:1 ratio) and a series of fluorescence and differential interference contrast frames were captured using a TCS SP5 confocal laser scanning unit attached to an inverted epifluorescence microscope (DMI6000) fitted with an HCX PL APO ×63/1.40–0.6 oil objective. Images were acquired and processed with the accompanying confocal software (LCS; Leica).

Activating planar lipid bilayers were formed in FCS2 flow chambers as previously described (Grakoui *et al*, 1999; Carrasco *et al*, 2004). Briefly, unlabelled GPI-linked ICAM-1 liposomes and biotinylated lipids were mixed with 1,2-dioleoyl-PC (DOPC) lipids (Avanti Polar Lipids, Inc.) to obtain the molecular density required. The chambers were then blocked with 2% FCS in PBS and loaded with streptavidin-labelled AlexaFluor-647, monobiotinylated T3b Ab as surrogate antigen. T cells were injected into the warmed chamber (37°C) at time zero, and were imaged with a Zeiss Axiovert LSM 510-META inverted microscope fitted with a ×40 oil objective and analysed with LSM 510 software (Zeiss, Germany) and ImageJ software.

For TIRFM, J77 T cells transfected with mitoYFP were allowed to settle onto CD3 plus CD28-coated coverslips in Attofluor open chambers (Invitrogen), and mitochondria were visualized with a Leica AM TIRF MC M mounted on a Leica DMI6000B microscope. Images were acquired and processed with the accompanying confocal software (LCS; Leica).

Assessment of mitochondrial membrane potential

The mitochondria-directed, fluorescent sensitive probe JC-1 was used to determine variations in mitochondrial membrane potential ($\Delta\psi_m$) (Solaini *et al*, 2007). The reversible formation of JC-1 aggregates upon membrane polarization was detected as a shift in emitted light from 520 nm (JC-1 monomeric form, FL1) to 590 nm (JC-1 aggregate, FL2). To assess $\Delta\psi_m$ in stimulated Jurkat T cells or T lymphoblasts, cells preloaded with JC-1 (2 μg/ml) were analysed by flow cytometry (FACScalibur, Becton Dickinson) and FL1 and

FL2 laser emissions were recorded (330 and 320 V, respectively). The mitochondrial depolarizing agent FCCP (250 nM) was used as a positive control.

$\Delta\psi_m$ of single mitochondria was assessed as described (Twig *et al*, 2008). Briefly, mitoYFP-transfected T cells were loaded with 50 nM TMRM, washed twice and allowed to settle on CD3 plus CD28 Ab-coated coverslips. A single *Z*-confocal plane was acquired, corresponding to the cell contact with the activating surface, with a TCS SP5 confocal microscope. For every time point, the TMRM and mitoYFP fluorescences were used to determine changes in $\Delta\psi_m$ using the accompanying confocal software (LCS, Leica).

Calcium measurement in T cell–APCs conjugates

J77 cells were loaded with Fluo-4 AM (2 μM) in HBSS containing 20 mM HEPES for 30 min at 37°C washed in 10% FCS RPMI medium and then in HBSS containing 20 mM HEPES and 1% FCS. Cells in 20 mM HEPES, 1% FCS HBSS were settled onto MatTek glass bottom dishes and CMAC-loaded Raji APCs were added at a 1:1 ratio. After 1 min of baseline recording, images were acquired every 15 s, using a TCS SP5 confocal laser scanning unit attached to an inverted epifluorescence microscope (DMI6000) fitted with an HCX PL APO ×40/1.40–0.6 oil objective. The 488-nm argon laser line was used to excite fluo4 fluorescence, which was measured using a band-pass filter from 505 to 550 nm and digitized to 12-bit resolution. Images were acquired and processed with the accompanying confocal software (LCS; Leica). The results are expressed as the fold increase in mean Fluo4 fluorescence intensity relative to the time before the T–APC stable contact. Ionomycin (0.5 μg/ml) was used as a positive control.

Flow cytometry

To track intracellular calcium levels, cells were incubated with Indo-1 (5 μg/ml) in prewarmed HBSS containing 10 mM HEPES and 1% FCS. After 30 min at 37°C cells were washed and resuspended in HBSS containing 1% FCS, and protected from light at room temperature for 15 min. Prewarmed cells were activated with CD3 Ab (10 μg/ml). Ca_i^{2+} flux was measured as the ratio of emission at 395–415 nm to 500–520 nm over time using an FACSCanto system (BD Biosciences), and analysed with Flow-Jo Software. Ionomycin (0.5 μg/ml) was used as a positive control.

ATP content was analysed in control and Drp1-silenced cells. Cells stimulated with CD3 plus CD28 Abs were treated with vehicle or oligomycin (4 μM). Cells were then stained with MgGr AM ester (5 μM) for 30 min. Emission intensity of the probe increases as a function of free Mg^{+2}, but decreases with ATP content.

Electron microscopy

Mitotracker Orange-loaded T cells, treated with vehicle (DMSO) or mdivi-1 inhibitor for 4 h, were conjugated with CMAC-loaded, SEE-pulsed Raji cells (APC) for 30 min on poly-L-Lys-coated coverslips (Bellco). Conjugates were fixed in 2.5% glutaraldehyde (Sigma-Aldrich) in PBS for 15 min, washed, and treated with 1% osmium tetroxide (Sigma-Aldrich) for 45 min. Samples were extensively washed with water and dehydrated through increasing concentrations of ethanol (25%, 50%, 75%, 95% and absolute). Samples were then embedded in DURCUPAN resin (Fluka) and stored overnight at room temperature. The resin column was polymerized by baking at 60°C for 48 h, and ultrathin sections were cut and contrasted. Sections were examined with a JEOL JEM1010 electron microscope (100 KV) equipped with a BioScan digital camera (Gatan). Images were monitored with DigitalMicrograph 3.1 (Gatan). T-cell mitochondria perimeter, area and distance from the IS were analysed with ImageJ software.

Statistical analysis

Data were tested for normality using the D'Agostino-Pearson omnibus normality test, or the Kolmogorov–Smirnov test when the sample was small due to experimental conditions. Differences between means were tested by Student's *t*-test for normal data, whereas non-normal data were analysed by the Mann–Whitney test. Data from multiple groups were analysed by ANOVA followed by Newman–Keuls multiple comparison test.

Supplementary data

Supplementary data are available at *The EMBO Journal* Online (http://www.embojournal.org).

Acknowledgements

We thank S Bartlett for editorial support and M Mittelbrunn, R González-Amaro, S Cadenas and JA Enríquez for critical reading of the manuscript. We also thank the technical support of C Aguado-Ballano and FR Urbano-Olmos (Universidad Autonoma de Madrid) during the TEM and the excellent support of the CNIC Microscopy and Celomics units. This work was supported by grants from the Spanish Ministry of Science and Innovation (SAF2008-02635), the Instituto Carlos III (Red RECAVA RD06/0014-0030), the Comunidad de Madrid (INSINET 0159/2006) and the Fundación CNIC to FSM, and PI070356 to JMS. GM was supported by the European Union-funded International Graduate Program in Molecular Medicine. The CNIC is supported by the Spanish Ministry of Science and Innovation and the Pro-CNIC Foundation.

Author contributions: FB, NBMC, GM, JMS and FSM designed the experiments and analysed the results; FB, NBMC, CCL, EV, YR and GM collected and analysed the data; and FB made the figures and wrote the manuscript with input from NBCM, JMS and FSM.

Conflict of interest

The authors declare that they have no conflict of interest.

References

Calabia-Linares C, Robles-Valero J, De La Fuente H, Perez-Martínez M, Martin-Cofreces NB, Alfonso-Pérez M, Gutierrez-Vázquez C, María Mittelbrunn M, Ibiza SU-O FR, Aguado-Ballano C, Sánchez-Sorzano CO, Sánchez-Madrid F, Veiga E (2011) Endosomal clathrin drives actin accumulation at the immunological synapse. *J Cell Sci* (doi:10.1242/jcs078832)

Campello S, Lacalle RA, Bettella M, Manes S, Scorrano L, Viola A (2006) Orchestration of lymphocyte chemotaxis by mitochondrial dynamics. *J Exp Med* **203:** 2879–2886

Carrasco YR, Fleire SJ, Cameron T, Dustin ML, Batista FD (2004) LFA-1/ICAM-1 interaction lowers the threshold of B cell activation by facilitating B cell adhesion and synapse formation. *Immunity* **20:** 589–599

Cassidy-Stone A, Chipuk JE, Ingerman E, Song C, Yoo C, Kuwana T, Kurth MJ, Shaw JT, Hinshaw JE, Green DR, Nunnari J (2008) Chemical inhibition of the mitochondrial division dynamin reveals its role in Bax/Bak-dependent mitochondrial outer membrane permeabilization. *Dev Cell* **14:** 193–204

Cereghetti GM, Stangherlin A, Martins de Brito O, Chang CR, Blackstone C, Bernardi P, Scorrano L (2008) Dephosphorylation by calcineurin regulates translocation of Drp1 to mitochondria. *Proc Natl Acad Sci USA* **105:** 15803–15808

Chan DC (2006) Mitochondria: dynamic organelles in disease, aging, and development. *Cell* **125:** 1241–1252

Chang CR, Blackstone C (2010) Dynamic regulation of mitochondrial fission through modification of the dynamin-related protein Drp1. *Ann NY Acad Sci* **1201:** 34–39

Chen H, Chan DC (2005) Emerging functions of mammalian mitochondrial fusion and fission. *Hum Mol Genet* **14** (Spec No. 2)**:** R283–R289

Chen H, Chomyn A, Chan DC (2005) Disruption of fusion results in mitochondrial heterogeneity and dysfunction. *J Biol Chem* **280:** 26185–26192

Dustin ML, Olszowy MW, Holdorf AD, Li J, Bromley S, Desai N, Widder P, Rosenberger F, van der Merwe PA, Allen PM, Shaw AS (1998) A novel adaptor protein orchestrates receptor patterning and cytoskeletal polarity in T-cell contacts. *Cell* **94:** 667–677

Eura Y, Ishihara N, Yokota S, Mihara K (2003) Two mitofusin proteins, mammalian homologues of FZO, with distinct functions are both required for mitochondrial fusion. *J Biochem* **134:** 333–344

Fukushima NH, Brisch E, Keegan BR, Bleazard W, Shaw JM (2001) The GTPase effector domain sequence of the Dnm1p GTPase regulates self-assembly and controls a rate-limiting step in mitochondrial fission. *Mol Biol Cell* **12:** 2756–2766

Gomez TS, Billadeau DD (2008) T cell activation and the cytoskeleton: you can't have one without the other. *Adv Immunol* **97:** 1–64

Grakoui A, Bromley SK, Sumen C, Davis MM, Shaw AS, Allen PM, Dustin ML (1999) The immunological synapse: a molecular machine controlling T cell activation. *Science* **285:** 221–227

Hollenbeck PJ, Saxton WM (2005) The axonal transport of mitochondria. *J Cell Sci* **118:** 5411–5419

Huse M, Lillemeier BF, Kuhns MS, Chen DS, Davis MM (2006) T cells use two directionally distinct pathways for cytokine secretion. *Nat Immunol* **7:** 247–255

Huttenlocher A, Sandborg RR, Horwitz AF (1995) Adhesion in cell migration. *Curr Opin Cell Biol* **7:** 697–706

Ibiza S, Victor VM, Bosca I, Ortega A, Urzainqui A, O'Connor JE, Sanchez-Madrid F, Esplugues JV, Serrador JM (2006) Endothelial nitric oxide synthase regulates T cell receptor signaling at the immunological synapse. *Immunity* **24:** 753–765

Ilani T, Vasiliver-Shamis G, Vardhana S, Bretscher A, Dustin ML (2009) T cell antigen receptor signaling and immunological synapse stability require myosin IIA. *Nat Immunol* **10:** 531–539

Ishihara N, Nomura M, Jofuku A, Kato H, Suzuki SO, Masuda K, Otera H, Nakanishi Y, Nonaka I, Goto Y, Taguchi N, Morinaga H, Maeda M, Takayanagi R, Yokota S, Mihara K (2009) Mitochondrial fission factor Drp1 is essential for embryonic development and synapse formation in mice. *Nat Cell Biol* **11:** 958–966

James DI, Parone PA, Mattenberger Y, Martinou JC (2003) hFis1, a novel component of the mammalian mitochondrial fission machinery. *J Biol Chem* **278:** 36373–36379

Koshiba T, Detmer SA, Kaiser JT, Chen H, McCaffery JM, Chan DC (2004) Structural basis of mitochondrial tethering by mitofusin complexes. *Science* **305:** 858–862

Kupfer A, Singer SJ (1989) Cell biology of cytotoxic and helper T cell functions: immunofluorescence microscopic studies of single cells and cell couples. *Annu Rev Immunol* **7:** 309–337

Lee KH, Dinner AR, Tu C, Campi G, Raychaudhuri S, Varma R, Sims TN, Burack WR, Wu H, Wang J, Kanagawa O, Markiewicz M, Allen PM, Dustin ML, Chakraborty AK, Shaw AS (2003) The immunological synapse balances T cell receptor signaling and degradation. *Science* **302:** 1218–1222

Li Z, Okamoto K, Hayashi Y, Sheng M (2004) The importance of dendritic mitochondria in the morphogenesis and plasticity of spines and synapses. *Cell* **119:** 873–887

MacAskill AF, Kittler JT (2010) Control of mitochondrial transport and localization in neurons. *Trends Cell Biol* **20:** 102–112

Malissen B (2003) Immunology. Switching off TCR signaling. *Science* **302:** 1162–1163

Martin M, Iyadurai SJ, Gassman A, Gindhart Jr JG, Hays TS, Saxton WM (1999) Cytoplasmic dynein, the dynactin complex, and kinesin are interdependent and essential for fast axonal transport. *Mol Biol Cell* **10:** 3717–3728

Martin-Cofreces NB, Robles-Valero J, Cabrero JR, Mittelbrunn M, Gordon-Alonso M, Sung CH, Alarcon B, Vazquez J, Sanchez-Madrid F (2008) MTOC translocation modulates IS formation and controls sustained T cell signaling. *J Cell Biol* **182:** 951–962

McBride HM, Neuspiel M, Wasiak S (2006) Mitochondria: more than just a powerhouse. *Curr Biol* **16:** R551–R560

Mittelbrunn M, Molina A, Escribese MM, Yanez-Mo M, Escudero E, Ursa A, Tejedor R, Mampaso F, Sanchez-Madrid F (2004) VLA-4 integrin concentrates at the peripheral supramolecular activation complex of the immune synapse and drives T helper 1 responses. *Proc Natl Acad Sci USA* **101:** 11058–11063

Monks CR, Freiberg BA, Kupfer H, Sciaky N, Kupfer A (1998) Three-dimensional segregation of supramolecular activation clusters in T cells. *Nature* **395:** 82–86

Morris RL, Hollenbeck PJ (1993) The regulation of bidirectional mitochondrial transport is coordinated with axonal outgrowth. *J Cell Sci* **104** (Part 3)**:** 917–927

Pilling AD, Horiuchi D, Lively CM, Saxton WM (2006) Kinesin-1 and Dynein are the primary motors for fast transport of mitochondria in Drosophila motor axons. *Mol Biol Cell* **17:** 2057–2068

Quintana A, Schwindling C, Wenning AS, Becherer U, Rettig J, Schwarz EC, Hoth M (2007) T cell activation requires mitochondrial translocation to the immunological synapse. *Proc Natl Acad Sci USA* **104:** 14418–14423

Schwindling C, Quintana A, Krause E, Hoth M (2010) Mitochondria positioning controls local calcium influx in T cells. *J Immunol* **184:** 184–190

Smirnova E, Griparic L, Shurland DL, van der Bliek AM (2001) Dynamin-related protein Drp1 is required for mitochondrial division in mammalian cells. *Mol Biol Cell* **12:** 2245–2256

Solaini G, Sgarbi G, Lenaz G, Baracca A (2007) Evaluating mitochondrial membrane potential in cells. *Biosci Rep* **27:** 11–21

Taguchi N, Ishihara N, Jofuku A, Oka T, Mihara K (2007) Mitotic phosphorylation of dynamin-related GTPase Drp1 participates in mitochondrial fission. *J Biol Chem* **282:** 11521–11529

Tanaka A, Youle RJ (2008) A chemical inhibitor of DRP1 uncouples mitochondrial fission and apoptosis. *Mol Cell* **29:** 409–410

Twig G, Elorza A, Molina AJ, Mohamed H, Wikstrom JD, Walzer G, Stiles L, Haigh SE, Katz S, Las G, Alroy J, Wu M, Py BF, Yuan J, Deeney JT, Corkey BE, Shirihai OS (2008) Fission and selective fusion govern mitochondrial segregation and elimination by autophagy. *EMBO J* **27:** 433–446

Varadi A, Johnson-Cadwell LI, Cirulli V, Yoon Y, Allan VJ, Rutter GA (2004) Cytoplasmic dynein regulates the subcellular distribution of mitochondria by controlling the recruitment of the fission factor dynamin-related protein-1. *J Cell Sci* **117:** 4389–4400

Vardhana S, Choudhuri K, Varma R, Dustin ML (2010) Essential role of ubiquitin and TSG101 protein in formation and function of the central supramolecular activation cluster. *Immunity* **32:** 531–540

Varma R, Campi G, Yokosuka T, Saito T, Dustin ML (2006) T cell receptor-proximal signals are sustained in peripheral microclusters and terminated in the central supramolecular activation cluster. *Immunity* **25:** 117–127

Verstreken P, Ly CV, Venken KJ, Koh TW, Zhou Y, Bellen HJ (2005) Synaptic mitochondria are critical for mobilization of reserve pool vesicles at Drosophila neuromuscular junctions. *Neuron* **47:** 365–378

Vicente-Manzanares M, Sanchez-Madrid F (2004) Role of the cytoskeleton during leukocyte responses. *Nat Rev Immunol* **4:** 110–122

Wulfing C, Davis MM (1998) A receptor/cytoskeletal movement triggered by costimulation during T cell activation. *Science* **282:** 2266–2269

Zhu PP, Patterson A, Stadler J, Seeburg DP, Sheng M, Blackstone C (2004) Intra- and intermolecular domain interactions of the C-terminal GTPase effector domain of the multimeric dynamin-like GTPase Drp1. *J Biol Chem* **279:** 35967–35974

